

Article

Not peer-reviewed version

Severity of Hepatocyte Damage and Prognosis in Cirrhotic Patients Correlate with Hepatocyte Magnesium Depletion

[Simona Parisse](#) , [Alessandra Gianoncelli](#) , [Gloria Isani](#) , [Francesco Luigi Gambaro](#) , [Giulia Andreani](#) , [Emil Malucelli](#) , [Giuliana Aquilanti](#) , [Ilaria Carlomagno](#) , [Raffaella Carletti](#) , [Monica Mischitelli](#) , [Flaminia Ferri](#) , [Veronica Paterna](#) , [Quirino Lai](#) , [Gianluca Mennini](#) , [Fabio Melandro](#) , [Cira Di Gioia](#) , [Massimo Rossi](#) , [Stefano Iotti](#) , [Michela Fratini](#) , [Stefano Ginanni Corradini](#) *

Posted Date: 12 May 2023

doi: [10.20944/preprints202305.0927v1](https://doi.org/10.20944/preprints202305.0927v1)

Keywords: hepatocyte; liver; liver transplantation; MELD; MELDNa; transient receptor potential melastatin 7; TRPM7



Preprints.org is a free multidiscipline platform providing preprint service that is dedicated to making early versions of research outputs permanently available and citable. Preprints posted at Preprints.org appear in Web of Science, Crossref, Google Scholar, Scilit, Europe PMC.

Copyright: This is an open access article distributed under the Creative Commons Attribution License which permits unrestricted use, distribution, and reproduction in any medium, provided the original work is properly cited.

Disclaimer/Publisher's Note: The statements, opinions, and data contained in all publications are solely those of the individual author(s) and contributor(s) and not of MDPI and/or the editor(s). MDPI and/or the editor(s) disclaim responsibility for any injury to people or property resulting from any ideas, methods, instructions, or products referred to in the content.

Article

Severity of Hepatocyte Damage and Prognosis in Cirrhotic Patients Correlate with Hepatocyte Magnesium Depletion

Simona Parisse ¹, Alessandra Gianoncelli ², Gloria Isani ³, Francesco Luigi Gambaro ⁴, Giulia Andreani ³, Emil Malucelli ⁵, Giuliana Aquilanti ², Ilaria Carlomagno ², Raffaella Carletti ⁴, Monica Mischtelli ¹, Flaminia Ferri ¹, Veronica Paterna ¹, Quirino Lai ⁶, Gianluca Mennini ⁶, Fabio Melandro ⁶, Cira Di Gioia ⁴, Massimo Rossi ⁶, Stefano Iotti ^{5,7}, Michela Fratini ^{8,9} and Stefano Ginanni Corradini ^{1,*}

¹ Department of Translational and Precision Medicine, Sapienza University of Rome. Viale dell'Università 37. 00185, Rome, Italy.

² Elettra-Sincrotrone Trieste, Strada Statale 14-km 163,5 in AREA Science Park, Basovizza, 34149 Trieste, Italy.

³ Department of Veterinary Medical Sciences, Alma Mater Studiorum-University of Bologna, Via Tolara di Sopra 50, 50055-Ozzano dell'Emilia, 40064 Bologna, Italy.

⁴ Department of Radiological Sciences, Oncology and Pathological Anatomy, "Sapienza" University and Umberto I Polyclinic of Rome. Viale del Policlinico 155. 00161. Rome, Italy.

⁵ Department of Pharmacy and Biotechnology, University of Bologna, 40126 Bologna, Italy.

⁶ General Surgery and Organ Transplantation Unit, AOU Policlinico Umberto I, Sapienza University of Rome. Viale del Policlinico 155. 00161. Rome, Italy.

⁷ National Institute of Biostructures and Biosystems. Via delle Medaglie d'oro, 305. 00136 Rome, Italy.

⁸ CNR-Institute of Nanotechnology c/o Physics Department, Sapienza University of Rome. Piazzale Aldo Moro 7. 00185. Rome, Italy.

⁹ Laboratory of Neurophysics and Neuroimaging (NaN), IRCCS Fondazione Santa Lucia. Via ardeatina 306.00179 Rome, Italy.

* Correspondence: stefano.corradini@uniroma1.it

Abstract: We aimed to evaluate the magnesium content in human cirrhotic liver and its correlation with serum AST levels, expression of hepatocellular injury, and MELDNa prognostic score. In liver biopsies obtained at liver transplantation we measured the magnesium content in liver tissue in 27 cirrhotic patients (CIRs) and 16 deceased donors with healthy liver (CTRLs) by atomic absorption spectrometry and within hepatocytes in 15 CIRs using synchrotron-based X-ray Fluorescence Microscopy. In 31 CIRs and 10 CTRLs we evaluated the immunohistochemical expression in hepatocytes of the transient receptor potential melastatin 7 (TRPM7), a magnesium influx chanzyme also involved in inflammation. CIRs showed a lower hepatic magnesium content [117.2 (IQR 110.5-132.9) vs 162.8 (IQR 155.9-169.8) µg/g; p<0.001] and a higher percentage of TRPM7 positive hepatocytes [53.0 (IQR 36.8-62.0) vs 20.7 (10.7-32.8) %; p<0.001] than CTRLs. In CIRs, MELDNa and serum AST at transplant correlated: a) inversely with the magnesium content both in liver tissue and hepatocytes; b) directly with the percentage of hepatocytes stained intensely for TRPM7. The latter also directly correlated with worsening of MELDNa at transplant compared to waitlisting. Magnesium depletion and overexpression of its influx chanzyme TRPM7 in hepatocytes are associated with severity of hepatocyte injury and prognosis in cirrhosis. These data represent the pathophysiological basis for a possible beneficial effect of magnesium supplementation in cirrhotic patients.

Keywords: hepatocyte; liver; liver transplantation; MELD; MELDNa; transient receptor potential melastatin 7; TRPM7

1. Introduction

Magnesium (Mg) is the fourth most abundant cation in the human body (Ca > K > Na > Mg) and the second most abundant intracellular cation after potassium. About 99% of the total body Mg²⁺ is located in the intracellular milieu, while around 1% is present in blood and extracellular fluids [1,2].

The complex role of Mg in cell and tissue metabolism is multifactorial. Established evidence show that Mg acts mainly as a key signalling element in cell physiology. Therefore, the concept about Mg as electrolyte is simplistic and outdated [3–7]. Mg is involved in most metabolic and biochemical pathways and is required in a wide range of vital functions, as bone formation, neuromuscular activity, signalling pathways, bioenergetics, glucose, lipid and protein metabolism, DNA and RNA metabolism and stability, cell proliferation and differentiation [3–9]. The enzymatic databases list more than 600 enzymes with Mg indicated as cofactor, and additional 200 are reported in which Mg acts as an activator [10]. However, it should be specified that, since Mg interacts directly with the enzyme substrates, it is itself a substrate rather than a cofactor [5–7].

Mg deficiency has been documented in several pathological conditions since the end of the last century [11]. Serum Mg concentration does not reflect the amount of magnesium in different body tissues. Therefore, a normal concentration of serum Mg does not rule out Mg deficiency [12]. In the last decades, a great number of epidemiological, clinical, and experimental research papers have documented that hypomagnesemia and/or chronic Mg deficiency, may result in disturbances in nearly every organ/body, contributing to or exacerbating pathological consequences and causing potentially fatal complications [13,14].

It has been proposed that Mg depletion could be implicated in the pathogenesis and progression of chronic liver diseases [15,16]. This hypothesis is based on studies that have associated a low intake or depletion of Mg with liver disease severity, and the administration of Mg-containing compounds with the improvement of hepatic inflammation and fibrosis. In fact, in three large human studies, a low dietary Mg intake was associated with more severe hepatic fibrosis [17], increased mortality due to liver disease[18], and increased risk of non-alcoholic fatty liver disease[19]. Furthermore, in experimental studies, Mg depletion has been shown to: a) induce increased deposition of collagen in vivo in the liver of rats treated with CCL4 or with ethanol [20] ; b) induce lipid accumulation in hepatocytes, inflammation and ballooning in rat liver in vivo [21]; c) alter the respiratory and metabolic functions of hepatocyte mitochondria in vitro [22]. Finally, human studies have also shown a beneficial effect of Mg-containing compounds administration on serum aminotransferase activities of patients with alcoholic liver disease [23,24], obesity[25] or in the setting of drug-induced liver injury [26]. In agreement, other experimental studies have shown that the administration of Mg in different types of formulations in different models of liver damage has beneficial effects on hepatocyte death, hepatic inflammation, [27–30] and fibrosis [31,32]. Furthermore, experimental studies have shown that an antifibrotic mechanism of several Mg formulations is to inhibit hepatic stellate cells (HSC) activity [31,33,34].

To support the hypothesis that Mg depletion may be implicated in the pathogenesis and progression of chronic liver disease, it would also be necessary to demonstrate that tissue Mg content is low in these patients and progressively decreases with increasing the disease severity. As for the studies performed on humans, most of them [35–40], although not all [41,42], found lower blood concentrations of Mg in cirrhotic patients than in healthy controls. Similarly, most [38,40,43,44], but not all [35,37,42] studies found a progressive reduction in magnesemia that correlated with the worsening of cirrhosis. In a study using the Mg intravenous loading test, a body depletion of Mg was clearly demonstrated in advanced cirrhosis compared to healthy controls[36]. Accordingly, studies investigating the tissue content of Mg in cirrhotic patients found its depletion in sublingual epithelial cells [39], red blood cell, mononuclear and polymorphonuclear cells [35], and muscles [41,45]. As for the muscle depletion of Mg, it was also found in the presence of normal serum Mg concentrations [41] and correlated with the severity of the disease [45]. Only one study, conducted on pediatric patients with secondary cryptogenic or biliary cirrhosis[46], investigated the liver Mg content using atomic absorption spectrometry and found that it was reduced compared to subjects with healthy liver undergoing exploratory laparotomy, without correlation with serum Mg concentrations.

Regarding adult patients with cirrhosis of more frequent etiology, no data are available on the Mg content of the liver tissue as a whole and, as recently pointed out by Liu et al. [16], within the hepatocytes.

A major Mg cellular transport mechanism depends on the transient receptor potential melastatin-subfamily member 7 (TRPM7) chanzyme. TRPM7 is ubiquitously expressed, has an ion channel permeable to the divalent cations Mg^{2+} , Ca^{2+} and Zn^{2+} and also possesses a C-terminal α -kinase domain able to phosphorylate substrates and to regulate stability and localization of its own channel [47,48]. TRPM7 is widely involved in the cell cycle and metabolism, inflammation and various cell death processes [47,49] and, as regards the liver, hepatocellular necrosis, lobular inflammation, increased activity of serum aminotransferases, activation of hepatic stellate cells and fibrosis [50]. For these reasons, a relevant role of TRPM7 in the pathogenesis of liver disease and cirrhosis has been hypothesized [50,51]. TRPM7 expression has been demonstrated in rat hepatocyte cell lines, human hepatoma cells and, *in vivo*, in human hepatocytes, but has not been correlated with liver disease [52,53]. Therefore, in the present study we compared, in samples obtained at the time of liver transplantation, the Mg content in liver tissue and the hepatocyte expression of TRPM7 in healthy liver of donors and in hepatic cirrhotic tissue obtained from adult patients. In cirrhotic patients, we also correlated tissue and hepatocyte Mg content and hepatocyte TRPM7 expression with a widely used disease prognostic index, the MELDNa score, and with an index of hepatocyte damage such as serum aminotransferase activity [54].

2. Materials and Methods

2.1. Study design

This is a single-center retrospective study relating Mg content in liver and hepatocytes and TRPM7 expression in hepatocytes to clinical data of patients with cirrhosis who underwent liver transplantation at the Sapienza University of Rome, Azienda Ospedaliero Universitaria Policlinico Umberto I, Rome, Italy. The study was performed in accordance with the Declaration of Helsinki and approved by the Ethics Committee of Sapienza University - Policlinico Umberto I (Ref. No.1129/14.12.06).

2.2. Study population and data collection

Samples of cirrhotic liver tissue taken at the time of liver transplantation from 58 patients were retrospectively analyzed. Exclusion criteria were acute or chronic liver failure, age >70 years, magnesium supplementation, estimated glomerular filtration rate <50 , alcohol intake discontinued for <6 months, treatment with vitamin D, calcium or bisphosphonates and thyroid disease. Twenty-six liver samples without steatosis obtained from deceased donors were analyzed as healthy liver controls.

Wedge liver biopsies were performed on the left hepatic lobe immediately after liver explant of cirrhotic livers and before ischemia in donors. The cirrhotic study population was divided according to the availability of snap frozen samples or formalin-fixed paraffin sections. In 27 cirrhotic patients (study population A) and 16 deceased liver donors in whom snap frozen liver biopsy was available, we measured the tissue Mg content by atomic absorption spectroscopy (Figure 1). In 31 cirrhotic patients (study population B) and 10 deceased liver donors in whom paraffin-preserved liver biopsy was available, we measured the cytoplasmic expression of TRPM7 in hepatocytes by immunohistochemistry. Furthermore, in 15 of the cirrhotic patients of study population B, we measured the intrahepatocellular Mg content at the TwinMic beamline of Elettra Synchrotron in Trieste 65 and, in 7 of these, also at the X-ray Fluorescence (XRF) beamline 66 at the same synchrotron facility.

Demographic and clinical data of cirrhotic patients were retrospectively collected from outpatient and hospitalization records at the time of transplantation. Data regarding deceased liver donors were collected from medical records at the time of transplantation. All measurements performed on cirrhotic livers were performed blinded to patient demographic and clinical variables.

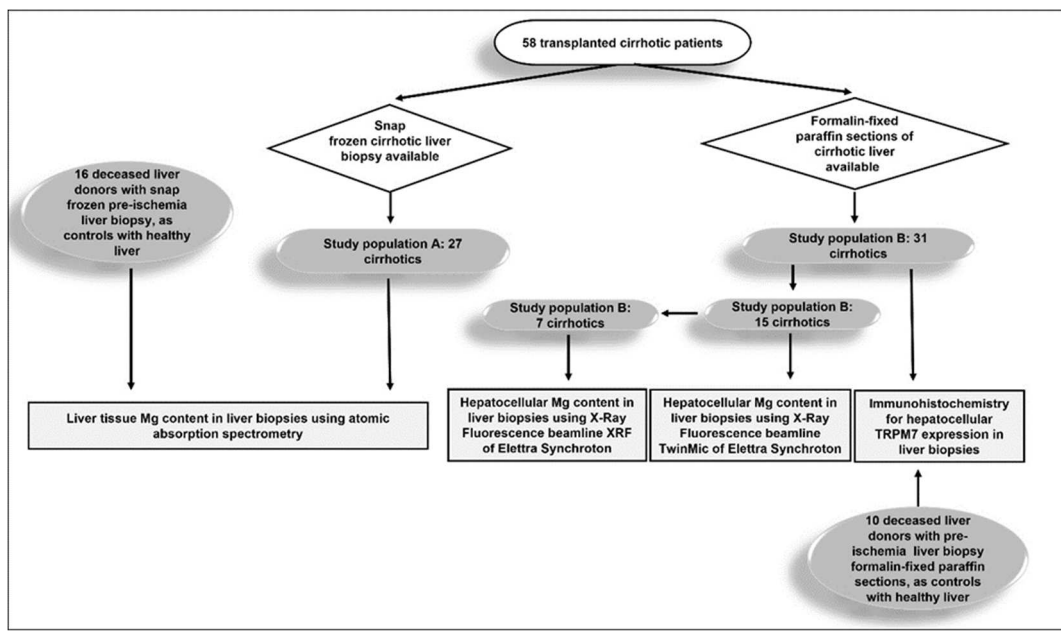


Figure 1. Schematic diagram depicting study populations of cirrhotic patients A and B and their respective healthy liver controls.

2.3. Magnesium quantification in liver tissue using atomic absorption spectrometry

To avoid contamination, polyethylene disposables were thoroughly washed with HCl 1 N under a fume hood, and disposable gloves were worn during the procedure. All the reagents were purchased from Merck (Merck-Sigma-Aldrich, Darmstadt, Germany); the acids were of Suprapur grade. Biopsies of liver tissue were placed in individual acid-washed teflon jars and were digested with 2 mL 65% HNO₃ and 0.5 mL 30% H₂O₂ in a microwave oven for 5 min at 250 W, 5 min at 400 W, 5 min at 500 W and 1 min at 600 W. The cooled samples were transferred into polyethylene volumetric flasks, diluted to 10 mL and directly analyzed using a flame atomic spectrophotometer equipped with a deuterium lamp background correction (AAnalyst 100, Perkin Elmer, Waltham, MA, USA) for Mg determination. All the samples were run in batches, which included blanks; there was no evidence of any contamination in these blanks. The accuracy of the method was evaluated using the analysis of international standards (ERM®-BB422 fish muscle). The concentrations found with the method used in this study fell into the certified uncertainty interval given by ERM, corresponding to a 95% confidence level. The Mg detection limit for flame atomic spectrophotometry was 0.04 µg mL⁻¹. Mg content in biopsies of liver tissue were reported as µg g⁻¹ wet weight (w.w.).

2.4. Determination of Magnesium in hepatocytes by Synchrotron Based X-ray Fluorescence Microscopy

Synchrotron based X-ray Fluorescence Microscopy to assess hepatocellular Mg content was performed using paraffin-embedded sections. Consecutive sections of the same specimen were used to obtain hematoxylin-eosin and 4 µm thick ultralene-mounted sections for XRFM analyses. To retrieve information at sub-cellular level low energy micro-X-ray Fluorescence (microXRF) measurements [57] combined with scanning transmission X-ray microscopy were carried out at TwinMic beamline [55]. The incident X-ray beam energy was set to 1.5 keV to ensure the best excitation and detection of the K_α lines of Mg and Na atoms. The samples were raster-scanned with step size of 1 µm across a microprobe of 1 µm diameter delivered perpendicularly to the sample plane by a 600 µm diameter Au zone plate optics with 50 nm outermost zone. 8 Silicon Drift Detectors located at 20 degrees in respect to the sample plane collected the XRF photons emitted by the sample [58] while a fast readout CCD camera acquired the transmitted X-ray photons producing simultaneous absorption and differential phase contrast images of the analysed areas [59]. All experiments were performed in high vacuum (HV) condition (10⁻⁶ mbar). The regions of interest were selected by inspecting the eosin and hematoxylin stained sections of the corresponding tissues.

Further XRFM analyses were performed at the XRF beamline on bigger samples' areas and a spatial resolution of about 100 microns to obtain information on more extended region, increasing the statistical value of the results. At the XRF beamline the samples were loaded in an Ultra HV chamber [60]. The beam energy was selected with a multilayer mirror, and the X-ray intensity was monitored using a polycrystalline diamond plate developed by the Elettra electronics group. The beam size was set to $200 \times 100 \mu\text{m}^2$ (Horizontal x Vertical) and the X-ray fluorescence emission was measured in 45/45 geometry using a Bruker XFlash 5030 detector placed at 15 mm from the samples. The samples were raster scanned using a seven-axes manipulator across an incident beam of 2.2 keV, to better enhance the X-ray fluorescence emission of Mg. All XRF spectra were then processed with PyMCA software [61]. Mg hepatocellular content were reported as X-ray Fluorescence counts.

2.5. Immunohistochemistry analysis for TRPM7 in hepatocytes

Immunohistochemical analysis for TRPM7 liver tissue expression was performed using paraffin-embedded sections. Consecutive sections of the same specimen were used to obtain hematoxylin-eosin and immunohistochemical stains. Immunohistochemical staining for TRPM7 (AbCam, ACC-047 clone) was routinely performed on the Leica Bond platform, according to manufacturer's instructions. Parotid gland normal tissue was used as positive control. Semiquantitative analysis of hepatocellular TRPM7 was conducted after identifying high expression, low expression and average expression areas of each specimen. In each one of these areas we identified the most representative high power field in which the percentage of weakly and strongly positive hepatocytes was recorded. For each sample, the average of the three analyzed areas of the percentages of high and low positive staining cells was determined. The same evaluation method was implemented in our study group and in organ donors. Hepatocytes stained mostly in a "dot like" cytoplasmic pattern, which was the object of our evaluation, with partial membrane and weak nuclear staining, which were considered inconsistent and consequently left out.

2.6. Statistical analysis

No missing data relative to study variables were observed. Data are presented as medians and interquartile ranges (IQR) for continuous variables and as numbers and percentages for discrete variables. For continuous variables, the normality was assessed by the Shapiro-Wilk test. The differences between two groups were evaluated by Mann-Whitney U test or t-test and the chi-squared test or Fisher's exact test, as appropriate. Pearson correlation coefficient was calculated to evaluate the correlation between clinical patients' data and Mg liver or hepatocellular content or hepatocellular TRPM7 expression. Hepatic Mg content and TRPM7 expression were investigated in relation to serum aminotransferase activity and, for cirrhotic patients, MELDNa measured at the time of liver transplantation [54]. In cirrhotic patients, the MELDNa data was available not only at the time of liver transplant but also at the time of waitlisting, allowing the calculation of Δ -MELDNa. Δ -MELDNa was calculated with the following formula: Δ -MELDNa = ((MELDNa at transplant - MELDNa at listing) / time elapsed between listing and transplant expressed in days) *100. In this way, positive Δ -MELDNa values mean that MELDNa, and therefore the patient's prognosis, at the time of transplantation were worse than at the time of listing, while Δ -MELDNa negative values indicate a clinical improvement during the time spent in the waiting list. Since MELDNa and serum AST activity at transplant and Δ -MELDNa were correlated, in the two investigated study population groups of cirrhotic patients, risk factors for increased MELDNa and serum AST at transplant and Δ -MELDNa were explored using separate multivariable linear regression models. In all models we included as initial independent covariates those significantly associated with the dependent variable and those that in other studies have been shown to be associated with serum Mg concentration. The variables to use for constructing the models were preliminarily selected using a Least Absolute Shrinkage and Selection Operator (LASSO) regression (stepwise regression with backward elimination), with the intent to create parsimonious models in terms of number of covariates [62]. After having identified the variables to analyze in the models by backward elimination, a 1000-fold bootstrap (resampling with replacement) method was used. Beta-coefficients and 95.0% confidence

intervals (95.0%CI) were reported. A P-value <0.05 was considered statistically significant. Statistical analyses were conducted using SPSS 27.0 (SPSS Inc., Chicago, IL, USA).

3. Results

3.1. In liver cirrhosis, hepatic magnesium content is lower and TRPM7 expression in hepatocytes is higher than in healthy liver.

Table 1 shows the demographic and clinical characteristics of cirrhotic patients in study populations A and B and their respective healthy liver donor control groups.

Table 1. Demographic and clinical characteristics of cirrhotic patients in study populations A and B and their respective healthy liver donor control group.

	Liver donors (controls of study population A)	Cirrhotic patients of study population A)	Liver donors (controls of study population B)	Cirrhotic patients of study population B)	P value liver donors (controls of study population A)	P value liver donors (controls of study population B)	P value cirrhotic patients study population A vs cirrhotic patients study population B)
Age, median (IQR)	16 53 (35-61.5)	27 52.0 (48.0-60.0)	10 62.5 (36.0-75.8)	31 57.3 (52.3-63.2)	0.890	0.984	0.050
Sex, male, n (%)	11 (68.8)	22 (81.5)	6 (60.0)	27 (87.1)	0.460	0.082	0.720
BMI (Kg/m2), median (IQR)	25.6 (24.8-27.3)	24.3 (22.6-27.4)	25.5 (24.2-27.6)	25.9 (24.4-29.0)	0.880	0.869	0.210
Cirrhosis aetiology, n (%):							
MAFLD	NA	16 (59.3)	NA	17 (54.8)	-	-	0.735
Alcohol		10 (37)		16 (51.6)			0.266
Viral		19 (70.4)		12 (38.7)			0.016
HCC, yes (%)	0 (0)	13 (48.1)	0 (0)	17 (54.8)	<0.001	<0.001	0.820
Diuretic treatment, n (%):							
None		8 (29.6)		11 (35.5)			
K sparing diuretics only	NAV	3 (11.1)	NAV	4 (12.9)	-	-	0.938
Loop diuretics plus K sparing diuretics		16 (59.3)		16 (51.6)			
Serum AST (IU/L), median (IQR)	35.5 (26.3-47.3)	63.0 (40.0-98.0)	52.5 (35.0-237.5)	59.0 (33.0-100.0)	0.873	0.665	0.925
Serum ALT (IU/L), median, (IQR)	23 (18-30.5)	47.0 (30.0-60.0)	67.0 (20.0-102.3)	43.0 (25.0-70.0)	0.792	0.665	0.911
MELDNA, at the time of liver transplant, median (IQR)	NA	18.0 (14.0-21.0)	NA	17.0 (12.0-26.0)	NA	NA	0.938
MELDNA, at the time of listing, median (IQR)	NA	15.7 (11.5-18.1)	NA	16.5 (12.0-23.4)	NA	NA	0.803
Days on the waiting list before liver transplant, median (IQR)	NA	128.0 (49.0-390.0)	NA	125.0 (50.0-186.0)	NA	NA	0.294
Δ-MELDNA, median (IQR)	NA	0.18 (0.00-1.28)	NA	0.92 (-0.31-3.43)	NA	NA	0.692

Abbreviations: AST aspartate amino transferase; ALT alanine amino transferase; BMI: body mass index; HCC, hepatocellular carcinoma; IQR, interquartile range; MAFLD, metabolic associated fatty liver disease; MELDNA, Model for End stage Liver Disease Sodium; K, potassium; Mg, magnesium; NA, not applicable; NAV, not available.

The only significant difference between the two populations of cirrhotic patients was the lower frequency of viral etiology of the disease in study population B compared to study population A, while no difference was present for age, sex, BMI, Metabolic associated fatty liver disease (MAFLD) and alcoholic etiology of cirrhosis, HCC, diuretic treatment, serum aminotransferase activities, MELDNa both at listing and at transplant, length of time on the waiting list and Δ -MELDNa. The two populations of cirrhotic patients did not differ from the respective healthy liver donor control groups for age, sex, BMI and serum aminotransferase activities. The median content of Mg, measured in biopsies of liver tissue using atomic absorption spectrometry, was significantly ($P < 0.001$) lower in cirrhotic patients of the study population A [117.2 (IQR 110.5-132.9) $\mu\text{g} / \text{g}$ w.w.] compared to its healthy liver donor controls group [162.8 (IQR 155.9-169.8) $\mu\text{g} / \text{g}$ w.w.] (Figure 2).

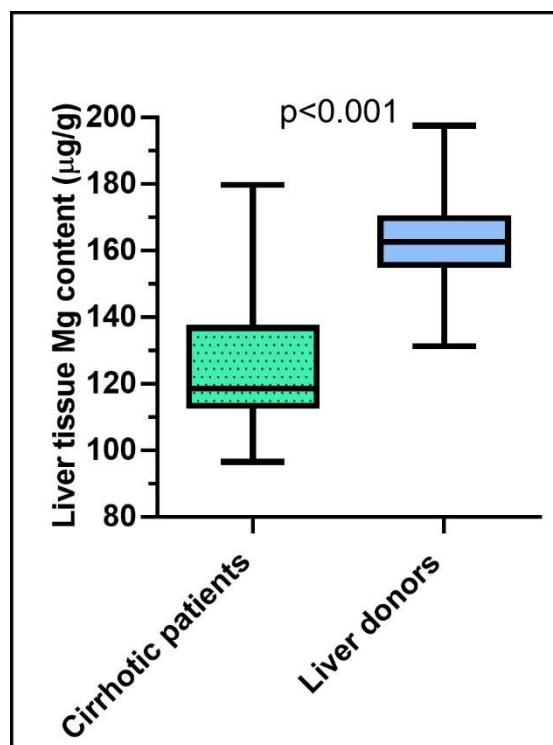


Figure 2. Box plots of the magnesium (Mg) content measured in liver biopsies using atomic absorption spectrometry in cirrhotic patients of study population A ($n=27$) and in the respective healthy liver donor control group ($n=16$).

Regarding TRPM7 expression, human salivary glands with highly positive cells with large cytoplasmic granules (Figure 3, panel A) were considered as a positive control. Then, we applied a semiquantitative scoring system by calculating the percentage of hepatocytes with intense or weak staining in cirrhotic and control donor livers. Considering cirrhotic liver samples from study population B (Figure 3 panels B, C), 81% showed intense staining in some hepatocytes, with up to 31% of hepatocytes affected. Weak staining affected all cirrhotic liver samples and 45% of these had at least half of the hepatocytes affected. In contrast, in donor control livers, only 30% of samples showed intense staining in some hepatocytes, with up to 3% of hepatocytes affected. Weak staining affected all donor liver samples but only 10% of these had at least half of the hepatocytes affected.

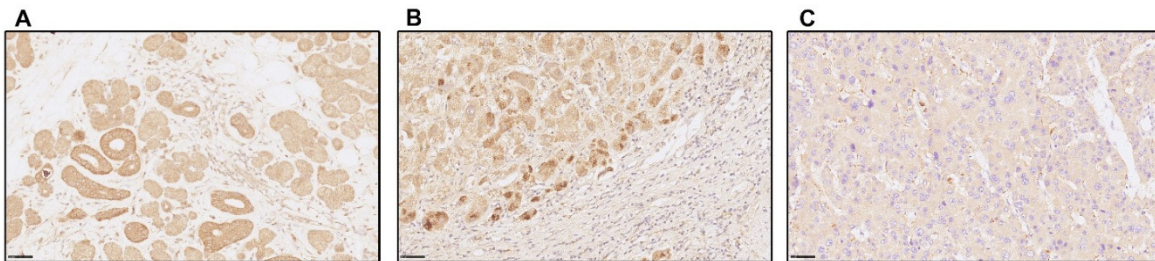


Figure 3. Representative immunohistochemistry images showing different expression patterns of transient receptor potential melastatin 7 (TRPM7) (40x; scale bars indicate 50 μ m). Panel A: Human salivary glands with positive cells with large cytoplasmic granules are shown as a positive control; panel B: Cirrhotic liver of study population B showing hepatocytes with intense granular cytoplasmic staining and others with weak staining; Panel C: Cirrhotic liver of study population B showing few weakly stained and most unstained hepatocytes.

The cirrhotic group of study population B, compared to its healthy liver donor control group, showed significantly higher percentages of hepatocytes with intense TRPM7 staining [2.8 (0.2-9.2) vs 0.0 (0.0-1.8)%; $p<0.01$], with weak staining [47.4 (34.0-56.2) vs 18.8 (10.7-32.8)%; $p<0.01$], and with total staining, i.e. weak or intense, [53.0 (36.8-62.0) vs 20.7 (10.7-32.8)%; $p<0.001$] (Figure 4 Panels A-C).

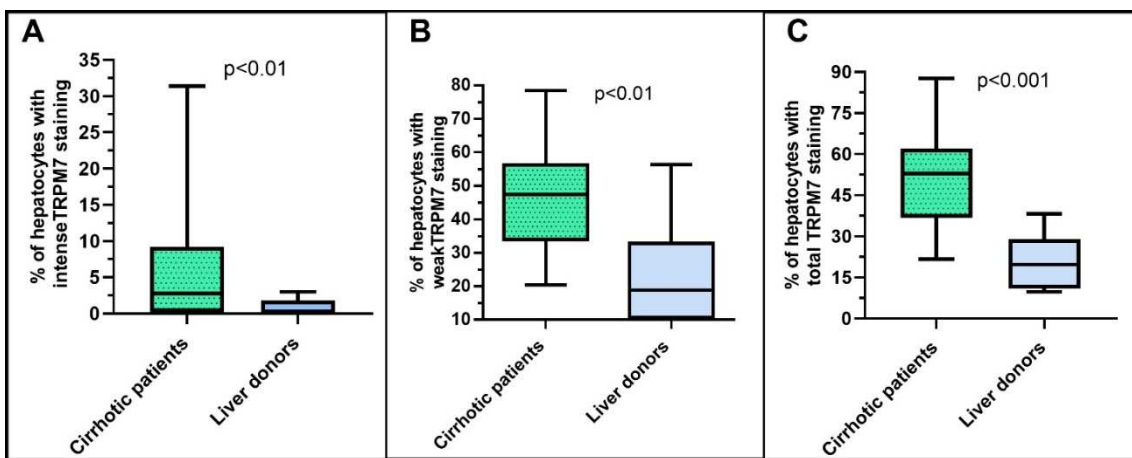


Figure 4. Box plots of the percentage of hepatocytes with TRPM7 expression in cirrhotic patients of study population B (n=31) and in the respective healthy liver donor control group (n=10) (panel A: intense expression; panel B weak expression; panel C total expression, i.e. intense and weak).

At least 4% of hepatocytes with intense TRPM7 staining were present in 45% of the cirrhotic liver samples and in none of the donor samples. Interestingly, in donor livers the percentage of TRPM7 positive hepatocytes was significantly lower ($p=0.01$) in those without any histological sign of inflammation [10.3 (IQR 8.4-13.3)%; n=4] versus those with mild inflammation [30.0 (IQR 21.2-43.6)%; n=6].

In liver cirrhosis, MELDNa at the time of liver transplantation is inversely correlated with the content of magnesium in liver tissue and hepatocytes and directly with the hepatocellular expression of TRPM7.

In cirrhotic patients of study population A, the MELDNa score measured at the time of liver transplant correlated inversely with the content of Mg measured in liver biopsies using atomic absorption spectrometry (Figure 5, panel A). To verify if this inverse correlation was retained, we used X-ray Fluorescence technique, an analytical method that allowed measuring Mg inside the hepatocytes in 15 cirrhotic patients of study population B. The significant inverse correlation between MELDNa and hepatocyte content of Mg measured at TwinMic beamline ($r = -0.531$; $p = 0.042$; Figure 5, panel B) and, in 7 of these patients, measured at XRF beamline ($r = -0.854$; $p = 0.014$) (Figure 5, panel C) was confirmed. Furthermore, the MELDNa score of study population B correlated directly with

the percentage of hepatocytes with intense and with total, i.e. sum of intense and weak, staining for TRPM7 (Figure 5, panels D and E). No correlation was found between MELDNa and the percentage of hepatocytes weakly stained for TRPM7.

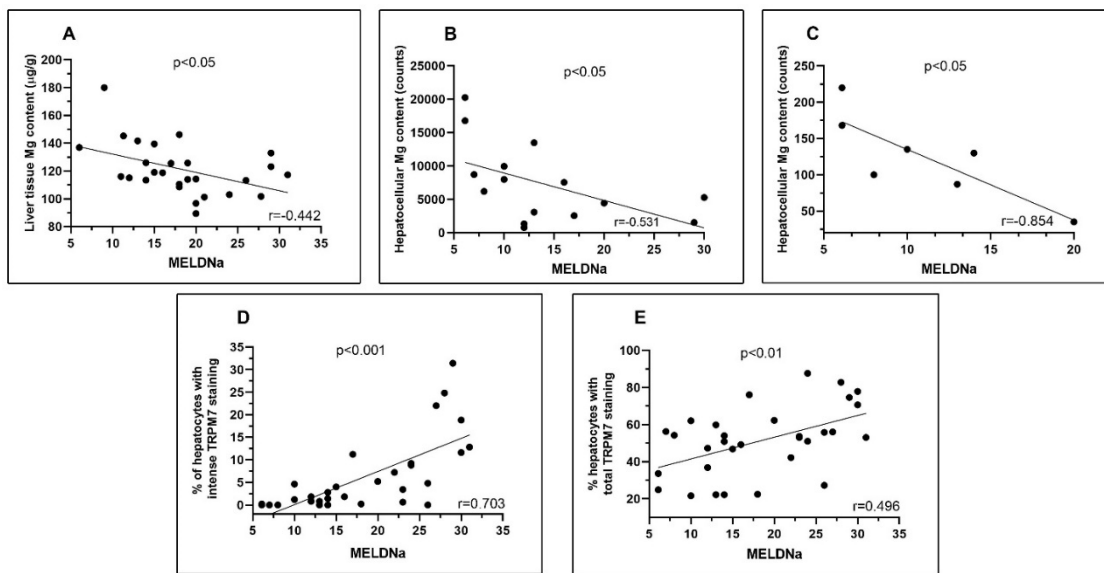


Figure 5. Correlation plots between MELDNa score of cirrhotic patients at liver transplant and the concentration of Mg measured in liver biopsies using atomic absorption spectrometry in study population A (panel A; n=27). Correlation plots between MELDNa score of cirrhotic patients at liver transplant and the hepatocyte content of Mg measured at Twinmic (panel B; n=15) or at XRF (panel C; n=7) beamlines of Elettra Synchrotron and the percentage of hepatocytes with intense (panel D; n=31) or total (panel E; n=31) TRPM7 staining in the study population B.

We then wanted to verify whether the correlations of the MELDNa values with Mg content in liver biopsies and with the hepatocellular expression of TRPM7 were independent of confounders. To do this we first analyzed whether, within each of the two cirrhotic study populations, patients differed when subgrouped into low and high MELDNa, based on their respective median MELDNa value (Table 2).

Table 2. Demographic and clinical characteristics of the cirrhotic patients of the study populations A and B, subgrouped according to the respective median of MELDNa.

	Cirrhotics of the study population A with low MELDNa	Cirrhotics of the study population A with high MELDNa	P value	Cirrhotics of the study population B with low MELDNa	Cirrhotics of the study population B with high MELDNa	P value
Age, median (IQR)	55.5 (48.2-62)	51 (45-56)	0.200	55.7 (52.3-63.8)	57.7 (52-61.9)	0.861
Sex, male, n (%)	10 (83.3)	12 (80)	1	14 (93.3)	13 (81.3)	0.600
BMI (Kg/m ²), median (IQR)	23.2 (22.6-30.6)	24.4 (23-26.9)	0.755	25.1 (24.4-29)	26.7 (23.5-28.9)	0.572
Cirrhosis aetiology, n (%):						
MAFLD	7 (58.3)	9 (60)	1	7 (46.6)	10 (62.5)	0.376
Alcohol	5 (41.6)	5 (33.3)	0.706	8 (53.3)	8 (50)	0.853
Viral	9 (75)	10 (66.6)	0.696	6 (40)	6 (37.5)	0.886
HCC, n (%)	11 (91.6)	3 (20)	<0.001	15 (100)	2 (12.5)	<0.001
Diuretic treatment, n (%):						
No						
K sparing diuretics only	6 (50)	2 (13.3)	0.031	8 (53.3)	3 (35.5)	0.001
Loop diuretics plus K sparing diuretics.	4 (33.3)	12 (80.0)		4 (26.7)	4 (12.9)	
	2 (6.7)	1 (6.7)		3 (20.0)	16 (51.6)	
MELDNa, median (IQR)	13.5 (11-15)	20 (19-27.8)	<0.001	12 (8-14)	22 (22.3-28.8)	<0.001

Serum AST (IU/L), median (IQR)	41(29-70)	90 (47-112)	0.007	35 (29-72)	84.5 (56.8-139.5)	0.005
Serum ALT (IU/L), median, (IQR)	37.5 (30.5-57)	51 (25-76)	0.456	36 (23-58)	53.5 (33.3-82)	0.119
Serum Mg, mg/dL, median (IQR)	NAV	NAV	-	1.9 (1.7-2.1)	1.9 (1.6-1.94)	0.318
Tissue Mg, (µg/g), median, (IQR) *	125.8 (116.8-141.1)	113.2 (101.7-123.2)	0.005	NAV	NAV	-
Percentage of weak positive hepatocytes to TRPM7 stain, median (IQR)	NAV	NAV	-	46.4 (26.4-54.2)	50.6 (36.3-57.8)	0.247
Percentage of intense positive hepatocytes to TRPM7 stain, median, (IQR)	NAV	NAV	-	0.8 (0-1.8)	9 (3.8-17.3)	<0.001
Percentage of total positive hepatocytes to TRPM7 stain, median (IQR)	NAV	NAV	-	47.2 (24.8-55)	55.9 (51.5-75.7)	0.014

* Measured by atomic absorption. All data refer to the time of liver transplant, unless otherwise specified.

Abbreviations: AST aspartate amino transferase; ALT alanine amino transferase; BMI: body mass index; HCC, hepatocellular carcinoma; IQR, interquartile range; MAFLD, metabolic associated fatty liver disease; MELDNa, Model for End stage Liver Disease Sodium; K, potassium; MELD, Mg, magnesium; NAV, not available; TRPM7, Transient Receptor Potential Cation Channel Subfamily M Member 7.

As expected, in the study population A, patients with high MELDNa had significantly lower Mg content than the low MELDNa group. In study population B, patients with high MELDNa showed a significantly higher proportion of hepatocytes with intense and total TRPM7 staining than those with low MELDNa. No intergroup difference in study population B was found with regard to the percentage of hepatocytes with weak TRPM7 expression. Furthermore, in both study populations A and B (Table 2), patients with lower MELDNa had a significantly higher frequency of HCC and a lower frequency of diuretic treatment compared with patients with higher MELD. No intergroup differences were present for age, sex, BMI and etiology of cirrhosis. The serum Mg concentration, available only for study population B, did not differ in patients with low compared to high MELDNa. The inverse correlation between MELDNa and the Mg content measured in liver biopsies and the direct correlations between MELDNa and the percentage of hepatocytes with intense or total TRPM7 staining were significant also performing multiple linear regression (Table 3).

Table 3. Multivariate linear regression analyses of variables associated with MELDNa in cirrhotic patients in the two study populations A and B.

		Independent variable	B	95% C.I. for B	P value
Study population A	Model 1 (Mg liver content measured by atomic absorption) *	Liver Mg content (ug/g)	-0.102	-0.207 – 0.005	0.048
		HCC, yes	-6.757	-10.785 – -2.571	0.008
Study population B	Model 2 (percentage of hepatocytes with intense TRPM7 expression) **	Percentage of hepatocytes with intense TRPM7 expression	0.297	0.175 - 0.578	0.005
		HCC, yes	-10.921	-13.683 - -8.046	0.001
	Model 3 (percentage of hepatocytes with total, i.e. weak and intense, TRPM7 expression) ***	Percentage of hepatocytes with total TRPM7 expression	0.101	0.023 - 0.179	0.021
		HCC, yes	-12.413	-15.274 - -9.923	0.001

Regression analyses data are shown only for significant associations after backward elimination and bootstrapping of the best model. *Model 1: age, HCC, diuretic treatment and Mg liver content measured by atomic absorption were introduced as covariates in the initial backward elimination model. **Model 2: age, presence of HCC, serum Mg concentration, diuretic treatment and the percentage of hepatocytes with intense TRPM7 expression were introduced as covariates in the initial backward elimination model. *** Model 3: age, presence of HCC, serum Mg concentration, diuretic treatment and the percentage of hepatocytes with total TRPM7 expression were introduced as covariates in the initial backward elimination model.

Finally, in the cirrhotic study population B, the serum Mg concentration correlated directly ($r = 0.553$; $P = 0.033$) with the Mg content in hepatocytes measured at the TwinMic beamline (Supplementary Figure S1), but did not correlate with any degree of TRPM7 expression. Furthermore, TRPM7 expression did not correlate with hepatic Mg content, measured at both Elettra Synchrotron TwinMic and XRF beamlines.

In liver cirrhosis, serum AST activity at the time of liver transplantation is inversely correlated with magnesium content in liver tissue and hepatocytes and directly with hepatocellular expression of TRPM7.

In cirrhotic patients of the group "study population A", the serum activity of AST at transplant, but not that of ALT, was inversely correlated with the Mg content measured in liver biopsies using atomic absorption spectrometry ($r = -0.458$; $p = 0.016$; Figure 6, panel A). In cirrhotic patients of study population B, the serum activity of AST at transplant, but not that of ALT, was inversely correlated with the content of Mg in hepatocytes measured using both the TwinMic ($r = -0.615$; $p = 0.015$; Figure 6, panel B) and XRF beamlines ($r = -0.758$; $p = 0.048$; Figure 6, panel C). In the cirrhotic patients of the group "study population B", serum activity of AST directly correlated with the percentage of both high intensity ($r=0.511$; $p=0.003$; Figure 5 panel D) and total ($r=0.428$; $p=0.016$; Figure 5 panel E), but not with the percentage of weakly TRPM7 positive hepatocytes. Serum activity of ALT directly correlated with the percentage of both high intensity ($r=0.439$; $p=0.013$) and total ($r=0.396$; $p=0.028$), but not with the percentage of weakly TRPM7 positive hepatocytes.

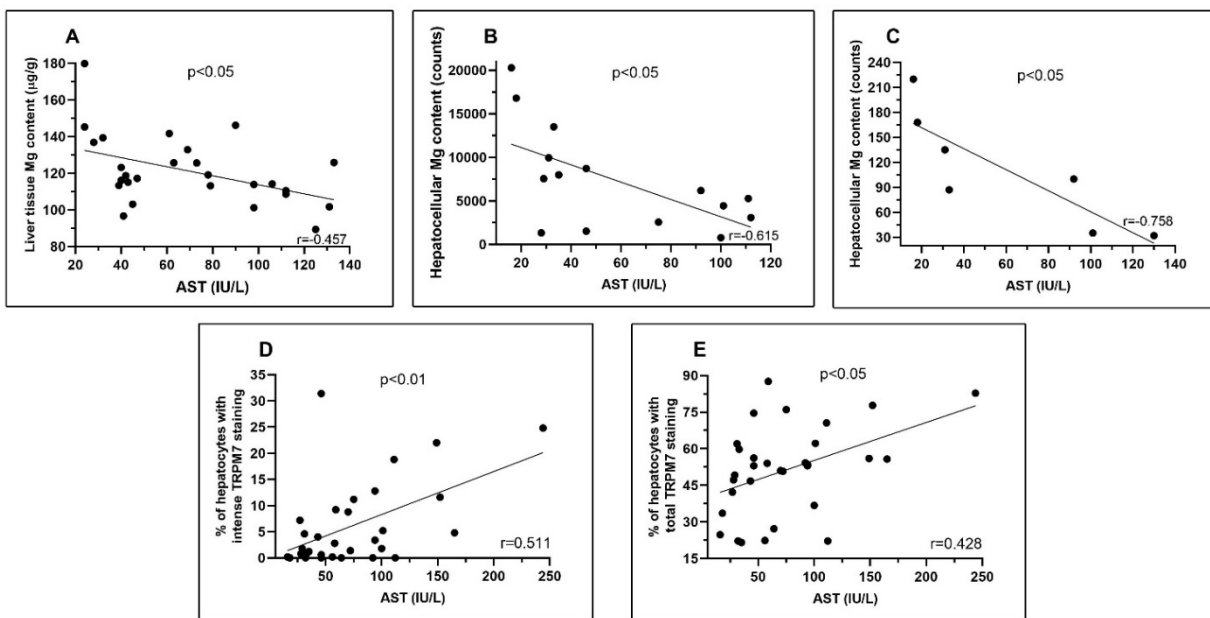


Figure 6. Correlation plots between serum AST activity of cirrhotic patients at liver transplant and the Mg content measured in liver biopsies using atomic absorption spectrometry in study population A (panel A; $n=27$). Correlation plots between serum AST activity of cirrhotic patients at liver transplant and their hepatocyte content of Mg measured at the TwinMic (panel B; $n=15$) or the XRF (panel C; $n=7$) beamlines of Elettra Synchrotron and the percentage of hepatocytes with intense (panel D; $n=31$) or total (panel E; $n=31$) TRPM7 staining in the study population B.

We then wanted to verify whether the correlations of the serum AST activity with Mg content in liver biopsies and with the hepatocellular expression of TRPM7 were independent of confounders. To do so we first analyzed whether, within each of the two cirrhotic study populations, patients differed in clinical and demographic characteristics when grouped according to the respective AST median value (Supplementary Table S1). In the group "study population A", the content of Mg measured in liver biopsies using atomic absorption spectrometry did not differ between the group with low and high AST serum activity. In the group "study population B", compared to patients with lower values, those having high AST activity showed a significantly higher percentage of hepatocytes with intense, but not weak or total TRPM7 staining. No intergroup differences were present for sex, BMI, etiology of cirrhosis and diuretic use in both study populations. The serum Mg concentration, available only for study population B, did not differ in patients with low compared to those with high serum AST. The inverse correlation between serum AST activity and the Mg content measured in liver biopsies and the direct correlation between AST serum activity and the percentage of hepatocytes with intense, but not total, TRPM7 staining remained significant even at multiple linear regression (Table 4).

Table 4. Multivariate linear regression analyses of variables associated with serum AST activity in cirrhotic patients in the two study populations.

		Independent variable	B	95% C.I. for B	P value
Study population A	Model 1 (Mg liver content measured by atomic absorption) *	Liver Mg content (ug/g)	-0.824	-1.560 - -0.288	0.007
		Age Years	-0.946	-2.209 – 0.763	0.155
Study population B	Model 2 (percentage of hepatocytes with intense TRPM7 expression) **	Percentage of hepatocytes with intense TRPM7 expression	3.256	0.758 – 6.208	0.040
		Age years	-2.787	-5.162 - -0.501	0.029
	Model 3 (percentage of hepatocytes with total, i.e. weak and intense, TRPM7 expression) ***	Percentage of hepatocytes with total TRPM7 expression	0.884	-0.078 – 1.958	0.114
		HCC, yes	-33.783	-65.886- -8.639	0.041

Regression analyses data are shown only for significant associations after backward elimination and bootstrapping of the best model. *Model 1: age, HCC, diuretic treatment, and Mg liver content measured by atomic absorption were introduced as covariates in the initial backward elimination model. **Model 2: age, presence of HCC, serum Mg concentration, diuretic treatment and the percentage of hepatocytes with intense TRPM7 expression were introduced as covariates in the initial backward elimination model. *** Model 3: age, presence of HCC, serum Mg concentration, diuretic treatment and the percentage of hepatocytes with total TRPM7 expression were introduced as covariates in the initial backward elimination model.

In liver cirrhosis the worsening of MELDNa during the waitlist time is inversely correlated with the content of magnesium in biopsies of liver tissue and directly with the hepatocellular expression of TRPM7 at the time of liver transplantation.

In cirrhotic patients, the MELDNa data were available not only at the time of liver transplant but also at the time of waitlisting, allowing the calculation of Δ -MELDNa. Δ -MELDNa correlated negatively with the content of Mg in liver biopsies measured using atomic absorption spectrometry in the group "study population A" ($r=-0.404$; $p=0.037$), while no significant correlation was found in study population B measuring Mg liver content at both TwinMic ($r=-0.367$; $p=0.178$) and XRF

beamlines ($r=-0.652$; $p=0.112$). In the cirrhotic patients of the group "study population B", Δ -MELDNA directly correlated with the percentage of both high intensity ($r=0.569$; $p=0.001$) and total ($r=0.402$; $p=0.025$), but not with the percentage of weakly stained, TRPM7 positive hepatocytes assessed at liver transplant.

We then wanted to verify whether the correlations of Δ -MELDNA with Mg content in liver biopsies measured using atomic absorption spectrometry and with the expression of TRPM7 were independent of confounders. To do so we first analyzed whether, within each of the two cirrhotic study populations, patients differed in clinical and demographic characteristics when grouped according to the respective Δ -MELDNA median value (Supplementary Table S2). In the group "study population A", the content of Mg measured in liver biopsies did not differ in the groups having low or high Δ -MELDNA. In study population B, patients with high compared to those with low Δ -MELDNA showed a significantly higher percentage of hepatocytes with intense and total, but not weak, TRPM7 staining. No intergroup differences were present for sex, BMI, etiology of cirrhosis and diuretic use in both study populations. The serum Mg concentration, available only for study population B, did not differ in patients with low compared to those with high Δ -MELDNA. At multiple linear regression introducing age, presence of HCC, serum Mg concentration, diuretic treatment as covariates in the initial backward elimination model, the direct correlation between Δ -MELDNA and the percentage of hepatocytes with intense ($B=0.436$; 95% CI of $B=0.179$ – 0.670 ; $P=0.009$) and with total TRPM7 staining ($B=0.153$; 95% CI of $B=0.054$ – 0.270 ; $P=0.025$) remained significant. On the contrary the Mg liver content was not significantly associated with Δ -MELDNA at multiple linear regression.

4. Discussion

In the present study, the median content of Mg measured in liver biopsies using atomic absorption spectroscopy at the time of liver transplantation, is about 1/3 lower in cirrhotic patients than in livers of healthy donor. This finding, obtained for the first time in adult patients with liver cirrhosis of common etiologies, is in agreement with a study performed in pediatric patients with secondary biliary cirrhosis or cryptogenic cirrhosis(46). A second important difference found in cirrhotic patients is that the median of the total percentage of hepatocytes expressing TRPM7 in the cytoplasm is 2.6 times higher than in healthy donors. Furthermore, nearly half of the cirrhotic liver samples but none of the donor samples had at least 4% of hepatocytes heavily stained for TRPM7.

Concerning cirrhotic patients, significant correlations were found between Mg content and TRPM7 expression in the liver on the one hand and simultaneously measured clinical variables on the other. In particular, the MELDNA and the serum AST activity of patients at the time of liver transplantation correlated inversely with the content of Mg measured both in the liver biopsies using atomic absorption and within the hepatocytes analysed by synchrotron microXRF. Furthermore, MELDNA and serum AST activity measured at transplant correlated directly with the total percentage of hepatocytes expressing TRPM7 and with the percentage of them with intense expression. The correlations between the Mg content in liver biopsies on the one hand and the intense expression of TRPM7 on the other hand with MELDNA and serum AST and the correlation between the total expression of TRPM7 and MELDNA were independent of some confounding factors known to influence blood or intracellular levels of Mg. These factors, included in the linear regression models as independent variables, were age [63], diuretic therapy [64], presence of HCC [65] and blood concentration of Mg, available only for models concerning the expression of TRPM7. The number of liver samples measured by synchrotron methods for the content of Mg in hepatocytes did not allow to perform multivariate analyses.

Taken together, our results demonstrate a close link between hepatocyte Mg metabolism and the presence and severity of liver cirrhosis. Regarding the progression of cirrhosis, we found close links between hepatocyte Mg metabolism and two simultaneously measured clinical indices, such as predominantly mitochondrial hepatocyte damage measured by serum AST and short-term prognosis of cirrhosis assessed by MELDNA. In particular, as the hepatic inflammation and the severity of the prognosis increased, the Mg content in hepatocytes decreased and the expression of TRPM7, which

facilitates the entry of Mg into these cells, increased. Strikingly then, the percentage of hepatocytes that, at the time of transplantation, strongly expressed TRPM7 was also associated with the recent time-dependent worsening of MELDNa during the waiting list.

Our hypothesis to explain these data is that, in cirrhosis, a hepatocellular Mg depletion occurs mainly caused by inflammation and that, in turn, the latter is increased by Mg depletion in a vicious circle similar to that demonstrated for the stressful situations [66]. This hypothesis is strongly supported by data, both in animal and human models, demonstrating that stress induces Mg depletion in erythrocytes. Although these studies were performed with non-inflammatory stress stimuli, inflammation definitely constitutes stress and therefore inflammation is likely to induce Mg depletion [66]. Indeed, also acute inflammation has been shown to cause cellular Mg depletion. This has been demonstrated in a mouse model of muscle damage and, with respect to the liver, in both mice and humans secondary to acetaminophen-induced liver damage[67–69]. According to our hypothesis, cellular Mg depletion caused by inflammation in turn aggravates the latter. Accordingly, many experimental studies have demonstrated that Mg depletion induces inflammation in different organs including the liver [21,68]. Among the multiple mechanisms by which Mg depletion can induce inflammation, the activation of TRPM7 can play an important role. Our data are in agreement with the previous demonstration of the presence of TRPM7 in human hepatocytes *in vivo*[53]. Hepatocyte Mg depletion causes TRPM7 overexpression to facilitate Mg entry into depleted cells [70]. However, TRPM7 activation is also able to stimulate inflammation and cell death, as demonstrated at several levels including the liver [47,49–51]. Noteworthy is that in our study we found a slight expression of TRPM7 in hepatocytes from donor livers in which mild inflammation was present. Previously, activation of TRPM7 only in hepatic stellate cells was thought to be responsible for liver fibrosis and elevation of serum aminotransferases in a mouse model of carbon tetrachloride-induced fibrosis [51]. Although we did not focus on hepatic stellate cells in the present study, we found a close association of clinical indices with TRPM7 activation in hepatocytes. Our results suggest that the administration of Mg in cirrhotic patients could interrupt the vicious circle between Mg depletion in the liver and hepatic inflammation and that it could reduce the expression of TRPM7 in these cells with beneficial effects. This is consistent with the beneficial effect of administration of Mg-containing compounds demonstrated by other studies in alcoholics, in obese patients, in patients with drug-induced liver injury, and in experimental models of liver damage[23–25,27,30–34].

A limitation of our study concerns its retrospective design. Furthermore, we analyzed two different populations of patients with liver cirrhosis due to the availability of liver tissue and its storage mode. This was different for tissue Mg content measurement using atomic absorption spectrometry on the one hand and for hepatocyte Mg content measured with XRFM and TRPM7 expression on the other hand. However, the fact that we found consistent results using two different analytical protocols to measure Mg in the liver, and at two different length scale, albeit in two different patient populations, strengthens our conclusions. In conclusion, in the present study we demonstrated that, *in vivo* in human liver affected by cirrhosis compared to normal liver, hepatocytes are Mg depleted and show an overexpression of TRPM7, channel for magnesium entry, which is probably secondary. Furthermore, the degree of Mg depletion correlates with serum levels of AST, a marker of hepatocyte death, and with MELDNa, a prognostic severity score. The degree of hepatocyte overexpression of TRPM7 in hepatocytes also correlates not only with serum AST levels and MELDNa, but also with the recent worsening of MELDNa over time. Finally, even in the normal liver TRPM7 is expressed in the presence of mild inflammation. These data suggest that Mg depletion and overexpression of TRPM7, which is known to have proinflammatory activity, may represent a therapeutic target in cirrhotic patients.

Supplementary Materials: The following supporting information can be downloaded at the website of this paper posted on Preprints.org.

Author Contributions: data interpretation and original draft preparation, S.P.; methodology and hepatocytes Mg content evaluation, A.G.; methodology and liver Mg content evaluation, G.I.; immunohistochemical staining readings F.L.G.; methodology and Liver Mg content evaluation G.A.; methodology and hepatocytes Mg content evaluation, E.M.; methodology and hepatocytes Mg content evaluation, G.Aq.; methodology and hepatocytes

Mg content evaluation, I.C.; methodology and immunohistochemical staining preparation, R.C.; clinical data collection, M.M.; clinical data collection and patient management, F.F.; data collection, V.P.; collection of liver samples, Q.L.; collection of liver samples, G.M.; collection of liver samples, F.M.; supervised the immunohistochemical staining, C.D.G.; supervision and liver transplantation, M.R.; conceptualization and revision of the manuscript, S.I.; conceptualization, methodology and revision of the manuscript, M.F.; conceptualization, data manager, statistical analysis and revision S.G.C.. All authors have read and critically reviewed the manuscript.

Funding: This research received no external funding

Institutional Review Board Statement: this study was approved by the Ethics Committee of Sapienza University - Policlinico Umberto I (Ref. No.1129/14.12.06).

Informed Consent Statement: Informed consent was obtained from all subjects involved in the study.

Data Availability Statement: Data are available upon request.

Conflicts of Interest: The authors declare no conflict of interest.

References

1. Schuchardt JP, Hahn A. Intestinal Absorption and Factors Influencing Bioavailability of Magnesium-An Update. *Curr Nutr Food Sci.* 2017 Nov;13(4):260–78.
2. Konrad M, Schlingmann KP, Gudermann T. Insights into the molecular nature of magnesium homeostasis. *Am J Physiol Renal Physiol.* 2004 Apr;286(4):F599-605.
3. Rubin H. Magnesium: The missing element in molecular views of cell proliferation control. *BioEssays.* 2005 Mar;27(3):311–20.
4. Kubota T, Shindo Y, Tokuno K, Komatsu H, Ogawa H, Kudo S, et al. Mitochondria are intracellular magnesium stores: investigation by simultaneous fluorescent imagings in PC12 cells. *Biochim Biophys Acta.* 2005 May 15;1744(1):19–28.
5. Iotti S, Frassineti C, Sabatini A, Vacca A, Barbiroli B. Quantitative mathematical expressions for accurate in vivo assessment of cytosolic [ADP] and DeltaG of ATP hydrolysis in the human brain and skeletal muscle. *Biochim Biophys Acta.* 2005 Jun 30;1708(2):164–77.
6. Feeney KA, Hansen LL, Putker M, Olivares-Yáñez C, Day J, Eades LJ, et al. Daily magnesium fluxes regulate cellular timekeeping and energy balance. *Nature.* 2016 Apr 21;532(7599):375–9.
7. Li FY, Chaigne-Delalande B, Kanellopoulou C, Davis JC, Matthews HF, Douek DC, et al. Second messenger role for Mg²⁺ revealed by human T-cell immunodeficiency. *Nature.* 2011 Jul 27;475(7357):471–6.
8. Sargent A, Castiglioni S, Olivi E, Bianchi F, Cazzaniga A, Farruggia G, et al. Magnesium Deprivation Potentiates Human Mesenchymal Stem Cell Transcriptional Remodeling. *Int J Mol Sci.* 2018 May 9;19(5).
9. Mammoli F, Castiglioni S, Parenti S, Cappadone C, Farruggia G, Iotti S, et al. Magnesium Is a Key Regulator of the Balance between Osteoclast and Osteoblast Differentiation in the Presence of Vitamin D3. *Int J Mol Sci.* 2019 Jan 17;20(2):385.
10. Caspi R, Billington R, Keseler IM, Kothari A, Krummenacker M, Midford PE, et al. The MetaCyc database of metabolic pathways and enzymes - a 2019 update. *Nucleic Acids Res.* 2020 Jan 8;48(D1):D445–53.
11. Whang R, Ryder KW. Frequency of hypomagnesemia and hypermagnesemia. Requested vs routine. *JAMA.* 1990 Jun 13;263(22):3063–4.
12. DiNicolantonio JJ, O'Keefe JH, Wilson W. Subclinical magnesium deficiency: a principal driver of cardiovascular disease and a public health crisis. *Open Heart.* 2018;5(1):e000668.
13. Martin KJ, González EA, Slatopolsky E. Clinical Consequences and Management of Hypomagnesemia. *Journal of the American Society of Nephrology.* 2009 Nov;20(11):2291–5.
14. Van Laecke S. Hypomagnesemia and hypermagnesemia. *Acta Clin Belg.* 2019 Jan 2;74(1):41–7.
15. Mathew AA, Panonnummal R. 'Magnesium'-the master cation-as a drug—possibilities and evidences. *BioMetals.* 2021 Oct 2;34(5):955–86.
16. Liu M, Yang H, Mao Y. Magnesium and liver disease. *Ann Transl Med.* 2019 Oct;7(20):578–578.
17. Tao MH, Fulda KG. Association of Magnesium Intake with Liver Fibrosis among Adults in the United States. *Nutrients.* 2021 Jan 2;13(1):142.
18. Wu L, Zhu X, Fan L, Kabagambe EK, Song Y, Tao M, et al. Magnesium intake and mortality due to liver diseases: Results from the Third National Health and Nutrition Examination Survey Cohort. *Sci Rep.* 2017 Dec 20;7(1):17913.
19. Lu L, Chen C, Li Y, Guo W, Zhang S, Brockman J, et al. Magnesium intake is inversely associated with risk of non-alcoholic fatty liver disease among American adults. *Eur J Nutr.* 2022 Apr 6;61(3):1245–54.

20. Rayssiguier Y, Chevalier F, Bonnet M, Kopp J, Durlach J. Influence of Magnesium Deficiency on Liver Collagen after Carbon Tetrachloride or Ethanol Administration to Rats. *J Nutr.* 1985 Dec;115(12):1656–62.
21. Fengler VH, Macheiner T, Goessler W, Ratzer M, Haybaeck J, Sargsyan K. Hepatic Response of Magnesium-Restricted Wild Type Mice. *Metabolites.* 2021 Nov 6;11(11):762.
22. Panov A, Scarpa A. Mg²⁺ Control of Respiration in Isolated Rat Liver Mitochondria. *Biochemistry.* 1996 Jan 1;35(39):12849–56.
23. Gullestad L, Dolva LO, Soyland E, Manger AT, Falch D, Kjekshus J. Oral Magnesium Supplementation Improves Metabolic Variables and Muscle Strength in Alcoholics. *Alcohol Clin Exp Res.* 1992 Oct;16(5):986–90.
24. Poikolainen K, Alho H. Magnesium treatment in alcoholics: A randomized clinical trial. *Subst Abuse Treat Prev Policy.* 2008 Dec 25;3(1):1.
25. Rodriguez-Hernandez H, Cervantes-Huerta M, Rodriguez-Moran M, Guerrero-Romero F. Oral magnesium supplementation decreases alanine aminotransferase levels in obese women. *Magnes Res.* 2010 Jun;23(2):90–6.
26. Wang Y, Wang Z, Gao M, Zhong H, Chen C, Yao Y, et al. Efficacy and safety of magnesium isoglycyrrhizinate injection in patients with acute drug-induced liver injury: A phase II trial. *Liver International.* 2019 Nov 21;39(11):2102–11.
27. Markiewicz-Górka I, Zawadzki M, Januszewska L, Hombek-Urban K, Pawlas K. Influence of selenium and/or magnesium on alleviation alcohol induced oxidative stress in rats, normalization function of liver and changes in serum lipid parameters. *Hum Exp Toxicol.* 2011 Nov 7;30(11):1811–27.
28. Cao Y, Shi H, Sun Z, Wu J, Xia Y, Wang Y, et al. Protective Effects of Magnesium Glycyrrhizinate on Methotrexate-Induced Hepatotoxicity and Intestinal Toxicity May Be by Reducing COX-2. *Front Pharmacol.* 2019 Mar 25;10.
29. Shafeeq S, Mahboob T. Magnesium supplementation ameliorates toxic effects of 2,4-dichlorophenoxyacetic acid in rat model. *Hum Exp Toxicol.* 2020 Jan 8;39(1):47–58.
30. Zhang Q, Zhou PH, Zhou XL, Zhang DL, Gu Q, Zhang SJ, et al. Effect of magnesium gluconate administration on lipid metabolism, antioxidative status, and related gene expression in rats fed a high-fat diet. *Magnes Res.* 2018 Nov 1;31(4):117–30.
31. Paik YH, Yoon YJ, Lee HC, Jung MK, Kang SH, Chung SI, et al. Antifibrotic effects of magnesium lithospermate B on hepatic stellate cells and thioacetamide-induced cirrhotic rats. *Exp Mol Med.* 2011 Jun 30;43(6):341–9.
32. El-Tantawy WH, Sabry D, Abd Al Haleem EN. Comparative study of antifibrotic activity of some magnesium-containing supplements on experimental liver toxicity. Molecular study. *Drug Chem Toxicol.* 2017 Jan 2;40(1):47–56.
33. Bian M, Chen X, Zhang C, Jin H, Wang F, Shao J, et al. Magnesium isoglycyrrhizinate promotes the activated hepatic stellate cells apoptosis via endoplasmic reticulum stress and ameliorates fibrogenesis *in vitro* and *in vivo*. *BioFactors.* 2017 Nov;43(6):836–46.
34. Pan X, Shao Y, Wang F, Cai Z, Liu S, Xi J, et al. Protective effect of apigenin magnesium complex on H₂O₂-induced oxidative stress and inflammatory responses in rat hepatic stellate cells. *Pharm Biol.* 2020 Jan 1;58(1):553–60.
35. Rocchi E, Borella P, Borghi A, Paolillo F, Pradelli M, Farina F, et al. Zinc and magnesium in liver cirrhosis. *Eur J Clin Invest.* 1994 Mar;24(3):149–55.
36. Koivisto M, Valta P, Höckerstedt K, Lindgren L. Magnesium depletion in chronic terminal liver cirrhosis. *Clin Transplant.* 2002 Oct;16(5):325–8.
37. Kar K, Dasgupta A, Vijaya Bhaskar M, Sudhakar K. Alteration of Micronutrient Status in Compensated and Decompensated Liver Cirrhosis. *Indian Journal of Clinical Biochemistry.* 2014 Apr 14;29(2):232–7.
38. Nangliya V, Sharma A, Yadav D, Sunder S, Nijhawan S, Mishra S. Study of Trace Elements in Liver Cirrhosis Patients and Their Role in Prognosis of Disease. *Biol Trace Elem Res.* 2015 May 24;165(1):35–40.
39. Cohen-Hagai K, Feldman D, Turani-Feldman T, Hadary R, Lotan S, Kitay-Cohen Y. Magnesium Deficiency and Minimal Hepatic Encephalopathy among Patients with Compensated Liver Cirrhosis. *Isr Med Assoc J.* 2018 Sep;20(9):533–8.
40. Peng X, Xiang R, Li X, Tian H, Li C, Peng Z, et al. Magnesium deficiency in liver cirrhosis: a retrospective study. *Scand J Gastroenterol.* 2021 Apr 3;56(4):463–8.
41. Chacko RT, Chacko A. Serum & muscle magnesium in Indians with cirrhosis of liver. *Indian J Med Res.* 1997 Nov;106:469–74.
42. Rahelić D, Kujundžić M, Romić Z, Brkić K, Petrovecki M. Serum concentration of zinc, copper, manganese and magnesium in patients with liver cirrhosis. *Coll Antropol.* 2006 Sep;30(3):523–8.
43. Chaudhry A, Toori KU, Shaikh JI. To determine correlation between biochemical parameters of nutritional status with disease severity in HCV related liver cirrhosis. *Pak J Med Sci.* 2018 Jan 16;34(1).

44. Llibre-Nieto G, Lira A, Vergara M, Solé C, Casas M, Puig-Diví V, et al. Micronutrient Deficiencies in Patients with Decompensated Liver Cirrhosis. *Nutrients*. 2021 Apr 10;13(4):1249.

45. AAGAARD NK, ANDERSEN H, VILSTRUP H, CLAUSEN T, JAKOBSEN J, DORUP I. Muscle strength, Na,K-pumps, magnesium and potassium in patients with alcoholic liver cirrhosis - relation to spironolactone. *J Intern Med*. 2002 Jul;252(1):56–63.

46. Göksu N, Özsoylu Ş. Hepatic and Serum Levels of Zinc, Copper, and Magnesium in Childhood Cirrhosis. *J Pediatr Gastroenterol Nutr*. 1986 May;5(3):459–62.

47. Zou ZG, Rios FJ, Montezano AC, Touyz RM. TRPM7, Magnesium, and Signaling. *Int J Mol Sci*. 2019 Apr 16;20(8):1877.

48. Cai N, Lou L, Al-Saadi N, Tetteh S, Runnels LW. The kinase activity of the channel-kinase protein TRPM7 regulates stability and localization of the TRPM7 channel in polarized epithelial cells. *Journal of Biological Chemistry*. 2018 Jul;293(29):11491–504.

49. Shi R, Fu Y, Zhao D, Boczek T, Wang W, Guo F. Cell death modulation by transient receptor potential melastatin channels TRPM2 and TRPM7 and their underlying molecular mechanisms. *Biochem Pharmacol*. 2021 Aug;190:114664.

50. Fang L, Zhan S, Huang C, Cheng X, Lv X, Si H, et al. TRPM7 channel regulates PDGF-BB-induced proliferation of hepatic stellate cells via PI3K and ERK pathways. *Toxicol Appl Pharmacol*. 2013 Nov;272(3):713–25.

51. Cai S, Wu L, Yuan S, Liu G, Wang Y, Fang L, et al. Carvacrol alleviates liver fibrosis by inhibiting TRPM7 and modulating the MAPK signaling pathway. *Eur J Pharmacol*. 2021 May;898:173982.

52. Ogunrinde A, Pereira RD, Beaton N, Lam DH, Whetstone C, Hill CE. Hepatocellular differentiation status is characterized by distinct subnuclear localization and form of the chanzyme TRPM7. *Differentiation*. 2017 Jul;96:15–25.

53. Badr H, Kozai D, Sakaguchi R, Numata T, Mori Y. Different Contribution of Redox-Sensitive Transient Receptor Potential Channels to Acetaminophen-Induced Death of Human Hepatoma Cell Line. *Front Pharmacol*. 2016 Feb 9;7.

54. Kim WR, Biggins SW, Kremers WK, Wiesner RH, Kamath PS, Benson JT, et al. Hyponatremia and Mortality among Patients on the Liver-Transplant Waiting List. *New England Journal of Medicine*. 2008 Sep 4;359(10):1018–26.

55. Gianoncelli A, Kourousias G, Merolle L, Altissimo M, Bianco A. Current status of the TwinMic beamline at Elettra: a soft X-ray transmission and emission microscopy station. *J Synchrotron Radiat*. 2016 Nov 1;23(6):1526–37.

56. Jark W, Grenci G. Focusing x-rays in two dimensions upon refraction in an inclined prism. In: Morawe C, Khounsary AM, Goto S, editors. *Proceedings of SPIE*. 2014. p. 92070A.

57. Gianoncelli A, Kaulich B, Alberti R, Klatka T, Longoni A, de Marco A, et al. Simultaneous soft X-ray transmission and emission microscopy. *Nucl Instrum Methods Phys Res A*. 2009 Sep;608(1):195–8.

58. Gianoncelli A, Kourousias G, Stolfa A, Kaulich B. Recent developments at the TwinMic beamline at ELETTRA: an 8 SDD detector setup for low energy X-ray Fluorescence. *J Phys Conf Ser*. 2013 Mar 22;425(18):182001.

59. Gianoncelli A, Morrison GR, Kaulich B, Bacescu D, Kovac J. Scanning transmission x-ray microscopy with a configurable detector. *Appl Phys Lett*. 2006 Dec 18;89(25):251117.

60. Karydas AG, Czyzycki M, Leani JJ, Migliori A, Osan J, Bogovac M, et al. An IAEA multi-technique X-ray spectrometry endstation at Elettra Sincrotrone Trieste: benchmarking results and interdisciplinary applications. *J Synchrotron Radiat*. 2018 Jan 1;25(1):189–203.

61. Solé VA, Papillon E, Cotte M, Walter Ph, Susini J. A multiplatform code for the analysis of energy-dispersive X-ray fluorescence spectra. *Spectrochim Acta Part B At Spectrosc*. 2007 Jan;62(1):63–8.

62. Simon Petersson, Klas Sehlstedt. Variable selection techniques for the Cox proportional hazards model: A comparative study. [Gothenburg]: University of Gothenburg; 2018.

63. Barbagallo M, Veronese N, Dominguez LJ. Magnesium in Aging, Health and Diseases. *Nutrients*. 2021 Jan 30;13(2):463.

64. Alexander RT, Dimke H. Effect of diuretics on renal tubular transport of calcium and magnesium. *American Journal of Physiology-Renal Physiology*. 2017 Jun 1;312(6):F998–1015.

65. Parisse S, Ferri F, Persichetti M, Mischitelli M, Abbatecola A, Di Martino M, et al. Low serum magnesium concentration is associated with the presence of viable hepatocellular carcinoma tissue in cirrhotic patients. *Sci Rep*. 2021 Jul 26;11(1):15184.

66. Pickering G, Mazur A, Trousselard M, Bienkowski P, Yaltsewa N, Amessou M, et al. Magnesium Status and Stress: The Vicious Circle Concept Revisited. *Nutrients*. 2020 Nov 28;12(12):3672.

67. Stankovic MS, Janjetovic K, Velimirovic M, Milenkovic M, Stojkovic T, Puskas N, et al. Effects of IL-33/ST2 pathway in acute inflammation on tissue damage, antioxidative parameters, magnesium concentration and cytokines profile. *Exp Mol Pathol.* 2016 Aug;101(1):31–7.
68. Castiglioni S, Cazzaniga A, Locatelli L, Maier JA. Burning magnesium, a sparkle in acute inflammation: gleams from experimental models. *Magnes Res.* 2017 Jan;30(1):8–15.
69. González-Recio I, Simón J, Goikoetxea-Usandizaga N, Serrano-Maciá M, Mercado-Gómez M, Rodríguez-Agudo R, et al. Restoring cellular magnesium balance through Cyclin M4 protects against acetaminophen-induced liver damage. *Nat Commun.* 2022 Nov 25;13(1):6816.
70. Shi R, Fu Y, Zhao D, Boczek T, Wang W, Guo F. Cell death modulation by transient receptor potential melastatin channels TRPM2 and TRPM7 and their underlying molecular mechanisms. *Biochem Pharmacol.* 2021 Aug;190:114664.

Disclaimer/Publisher's Note: The statements, opinions and data contained in all publications are solely those of the individual author(s) and contributor(s) and not of MDPI and/or the editor(s). MDPI and/or the editor(s) disclaim responsibility for any injury to people or property resulting from any ideas, methods, instructions or products referred to in the content.